Hindawi Publishing Corporation
Journal of Chemistry
Volume 2013, Article ID 460635, 8 pages
http://dx.doi.org/10.1155/2013/460635

Research Article

Biosorption of Ni(II), Cr(III), and Co(II) from Solutions Using Acalypha hispida Leaf: Kinetics, Equilibrium, and Thermodynamics

Adesola Babarinde,[1] J. Oyebamiji Babalola,[2] John Adegoke,[1] Adebola O. Osundeko,[1] Susan Olasehinde,[1] Adetayo Omodehin,[1] and Emmanuel Nurhe[1]

[1] *Department of Chemical Sciences, Olabisi Onabanjo University, Ago-Iwoye 120106, Nigeria*
[2] *Department of Chemistry, University of Ibadan, Ibadan 120106, Nigeria*

Correspondence should be addressed to Adesola Babarinde; solababarinde@yahoo.com

Received 26 June 2012; Accepted 10 August 2012

Academic Editor: Ana Cristi Basile Dias

Copyright © 2013 Adesola Babarinde et al. This is an open access article distributed under the Creative Commons Attribution License, which permits unrestricted use, distribution, and reproduction in any medium, provided the original work is properly cited.

Biosorption studies were conducted to study the removal of Ni(II), Cr(III), and Co(II) from aqueous solution of *Acalypha hispida* leaf. The FTIR spectral characteristics of *Acalypha hispida* leaf revealed the presence of ioniazable groups that could participate in the binding of metal ions in solution. The kinetic, equilibrium, and thermodynamic studies of the biosorption of the metal ions were investigated using various physicochemical parameters; each parameter was found to affect the biosorption process. The kinetic studies showed that the biosorption process was best represented by pseudo-second-order kinetics among four kinetic models tested. Equilibrium data were better represented by Freundlich isotherm among Langmuir and Freundlich adsorption isotherms. The study on the effect of dosage showed that the dosage of the biomass significantly affected the uptake of the metal ions from solution. Thermodynamic parameters such as standard Gibbs-free energy (ΔG°), standard enthalpy (ΔH°), standard entropy (ΔS°), and the activation energy (A) were calculated. The order of spontaneity of the biosorption process was found to be Cr(III) > Ni(II) > Co(II). The activation energy for the biosorption of each of the metal ions was less than 42 kJmol^{-1} at 323 K indicating that each was a diffusion-controlled process.

1. Introduction

Environmental pollution by toxic metals is a worldwide problem due to increased industrialisation. The metal ions are particularly problematic due to their accumulation in the food chain and their persistence [1]. Among the metal ions are Ni(II), Cr(III), and Co(II). There is the need to regulate their levels in the environment before they enter food chain. Of recent, biosorption of metal ions using biological materials has been identified as a potential technique for remediation of metal bearing effluents [2–11]. Biosorption has the merits of low cost and environmental friendliness over the conventional methods of removing metal ions from solution [6]. *Acalypha hispida* (Red Hot Cattails) is a plant that is native to the South Pacific (New Guinea and the Malay Archipelago). *Acalypha hispida* is a tropical shrub in the spurge family (Euphorbiaceae). This interesting plant gets its common name from the exotic flowers that look like strands of chenille yarn. Other descriptive common names include foxtails, monkey tail, red-hot cat's tail or chenille plant. It is usually grown as a houseplant for its unusual tassel-like flowers. This evergreen plant can grow to 15-feet tall and 8-feet wide in suitable climates but in containers will remain much smaller. *Acalypha hispida* flower has been reported to contain three anthocyanins, cyanidin 3-*O*-(2$''$-galloyl-6$''$-*O*-α-rhamnopyranosyl-β-galactopyranoside) (5%), cyanidin 3-*O*-(2$''$-galloyl-β-galactopyranoside) (85%), and cyanidin 3-*O*-β-galactopyranoside (5%) [12]. Phytochemical screening of the leaf extracts revealed the presence of tannin, alkaloid, steroid, saponin, and flavonoid [13]. It was on this basis that this readily available weed was investigated for its potential

in treating industrial effluents containing Ni(II), Cr(III), and Co(II) in the present study.

2. Methodology

2.1. Biomass Preparation. *Acalypha hispida* leaves were harvested from the mini campus of Olabisi Onabanjo University, Ago-Iwoye, Ogun State, Nigeria. The leaves were carefully collected inside a transparent nylon, sun dried immediately, and kept dry till time of usage.

2.2. Preparation of Solution. All chemicals used in this study were of analytical reagent grade and were used without further purification. Standard solutions of Ni(II), Cr(III) and Co(II) used for the study were prepared from $NiCl_2{\cdot}6H_2O$, $Cr(NO_3)_3{\cdot}9H_2O$, and $CoSO_4{\cdot}7H_2O$, respectively. The working solutions with different concentrations of the metal ions were prepared by appropriate dilutions of the stock solution immediately prior to their use with distilled water. The initial pH of the solution was adjusted accordingly with a pH meter. Thermostated Water bath (Haake Wia Model) was used as the medium for the process. The concentration before and after biosorption of each metal ion was determined using a Perkin-Elmer Analyst 700 flame atomic absorption spectrophotometer (AAS) with deuterium background corrector. Fourier transform infrared (FTIR) spectra of dried unloaded biomass and metal loaded biomass were recorded at 400–4000 cm^{-1} using a Shimadzu FTIR model 8400 S spectrophotometer.

2.3. Batch Biosorption Study. The biosorption study was determined by batch experiments by contacting 0.5 g of the *Acalypha hispida* leaf with 25 mL of each metal ion solution under different conditions for a period of time in a glass tube. The biosorption studies were conducted at 27°C using thermostated water bath to determine the effect of pH, contact time, and initial metal ion concentration on the biosorption. The residual metal ion of the supernatant was analyzed using AAS. The amount of metal ion biosorbed from solution was determined by difference and the mean value calculated.

2.4. Effect of pH on Biosorption. The effect of pH on the biosorption of the metal ion was carried out within pH 1–7 to prevent the precipitation of metal ions. This was done by contacting 0.5 g of *Acalypha hispida* leaf with 25 mL of 100 mgL^{-1} metal ion solution in a glass tube. The pH of each solution was adjusted to the desired value by drop wise addition of 0.1 M HNO_3 and/or 0.1 M NaOH. The glass tubes containing the mixture were left in a water bath for 6 hours. The biomass was removed from the solution by decantation. The residual metal ion concentration in the supernatant was analyzed. The optimum pH was determined as the pH with the highest biosorption of each metal ion.

2.5. Effect of Contact Time on Biosorption. The biosorption of the metal ions by *Acalypha hispida* leaf was studied at various time intervals (0–360 min) and at the concentration of 100 mgL^{-1}. This was done by contacting 0.5 g of *Acalypha hispida* leaf with 25 mL of 100 mgL^{-1} of metal ion solution at optimal pH. The leaf was left in solution for different periods of time. At predetermined time, the glass tubes were withdrawn from the bath, and the residual metal ion concentration in solution was determined using AAS. The amount of metal ions biosorbed was calculated for each sample.

2.6. Effect of Initial Concentration on Biosorption. Batch biosorption study of metal ion was carried out using a concentration range of 10–100 mgL^{-1}. This was done by contacting 0.5 g of the leaf with 25 mL of each solution at optimal pH. Two glass tubes were used for each concentration. The tubes were left in a thermostated water bath maintained at 27°C for the predetermined optimum time. The leaf was removed from the solution, and the concentration of residual metal ion in each solution was determined.

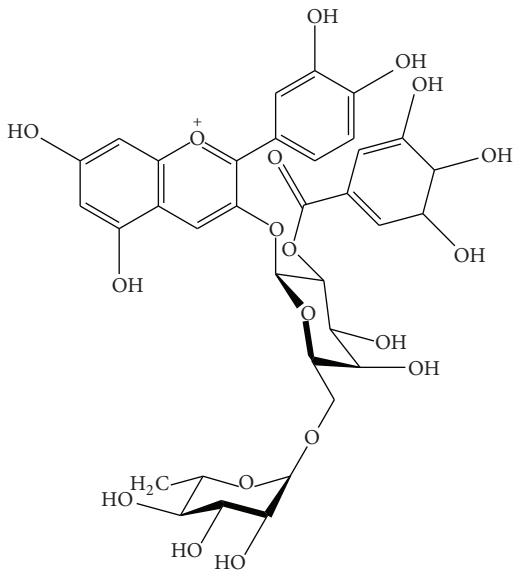
2.7. Effect of Temperature on Biosorption. The batch biosorption process was studied at different temperatures within the range 20–50°C in order to investigate the effect of temperature on the biosorption process. This was done by contacting 0.5 g of *Acalypha hispida* leaf with 25 mL of 100 mgL^{-1} of metal ion solution at the optimal pH and time.

2.8. Statistical Analyses. The curve fittings of the data obtained were performed using Microcal Origin 6.0 software.

3. Results and Discussion

3.1. Physical Characterization of Acalypha hispida. The biosorption capacity of *Acalypha hispida* leaf biomass depends upon the chemical reactivity of functional groups at the surface. Three anthocyanins including the novel pigment, cyanidin 3-*O*-(2-galloyl-6-*O*-α-rhamnopyranosyl-β-galactopyranoside), cyanidin 3-*O*-(2″-galloyl-β-galactopyranoside) (85%), and cyanidin 3-*O*-β-galactopyranoside (5%) have been isolated from the red flowers of *Acalypha hispida* [12]. The structure of cyanidin 3-*O*-(2-galloyl-6-*O*-α-rhamnopyranosyl-β-galactopyranoside) shows the presence of several ionisable groups that could participate in the biosorption of metal ions from solution (see Scheme 1) (1).

Phytochemical screening of the leaf extracts revealed the presence of tannin, alkaloid, steroid, saponin, and flavonoid [13, 14]. Therefore, knowledge of the surface functional groups would give insight to the biosorption capacity of the biomass. These groups would form active sites for sorption on the material surface. The FTIR spectra of dried unloaded and metal-loaded leaf were taken to obtain information on the nature of possible interactions between the functional groups of *Acalypha hispida* leaf biomass and the metal ions as presented in Figure 1. Several peaks were observed from the spectra indicating that *Acalypha hispida* leaf is composed of various functional groups which are responsible for binding of the cations. The IR spectra pattern of the biomass showed distinct and sharp absorptions indicative of the existence of the –OH, –NH, –C–O–, and C=O groups as shown in



Cyanidin 3-*O*-(2-galloyl-6-*O*-α-rhamnopyranosyl-β-galactopyranoside)

Scheme 1

Figure 1. These bands are due to the functional groups of *Acalypha hispida* leaf that participate in the biosorption of Ni(II), Cr(III), and Co(II). On comparison, there are clear band shifts and, decrease in intensity between the bands of the unloaded biomass and that of the metal-bound biomass as presented in Table 1. The FTIR spectra of the *Acalypha hispida* leaf biomass indicated slight changes in the absorption peak frequencies due to the fact that the binding of the metal ions causes reduction in absorption frequencies. These observed shifts in absorbance imply that there were metal binding processes taking place on the active sites of the biomass. Analysis of the FTIR spectra showed the presence of ionizable functional groups (O–H, NH_2, C–O, C=O,) which are able to interact with cations [1, 6, 15–17]. This implies that these functional groups would serve in the removal of positively charged ions from solution.

3.2. Effect of Solution pH on Metal Ion Biosorption. The pH of the solution usually plays an important role in the biosorption of the metal ions [18]. It is an important parameter governing the uptake of heavy metals by biosorption process as it not only affects metal species in solution, but also influences the surface properties of biosorbents in terms of dissociation of binding sites and surface charge [19]. The net charge of the sorbate and that of the sorbent are dependent on the pH of the solution. At low pH, the metal ion uptake is inhibited by net positive charge on the sorbent and the competition between the metal ions and the hydrogen ions in solution. As the pH increases, the negative charge density on biomass increases as a result of deprotonation of the metal binding sites on the biomass, consequently, the biosorption of the metal ions increases. Figure 2 shows the variation of the metal ions biosorbed on *Acalypha hispida* leaf at various solution pH values. For the three metal ions, the biosorption increased as the pH increased from pH 1 to pH 5. The increase observed

Table 1: The FT-IR spectral characteristics of *Acalypha hispida* leaf before and after biosorption of Ni(II), Cr(III), and Co(II).

Metal ion	FTIR absorption band peak (cm^{-1})			Assignment
	Before	After	Difference	
Ni(II)		1232.55	17.36	
Cr(III)	1215.19	1236.41	21.22	C–O stretch
Co(II)		1230.63	15.44	
Ni(II)		1442.8	−1.93	
Cr(III)	1444.73	1440.87	−3.86	O–H bend
Co(II)		1440.87	−3.86	
Ni(II)		1626.05	2.07	
Cr(III)	1624.12	1627.97	3.85	N–H bend
Co(II)		1626.05	1.93	
Ni(II)		1651.12	3.86	
Cr(III)	1647.26	1643.41	−3.85	C=O stretch
Co(II)		1643.41	−3.85	
Ni(II)		3321.53	7.71	
Cr(III)	3313.82	3323.46	9.64	O–H stretch
Co(II)		3313.82	0	
Ni(II)		3410.26	7.72	
Cr(III)	3402.54	3398.9	−3.64	N–H stretch
Co(II)		3417.98	15.44	

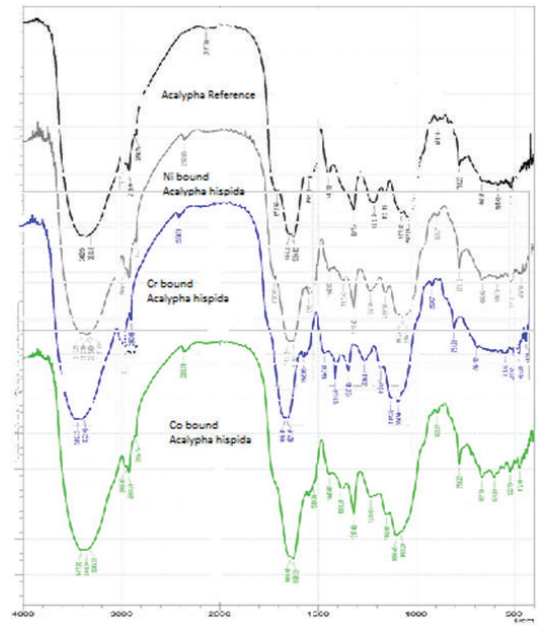


Figure 1: FTIR spectra of the free and metal-bound *Acalypha hispida* leaf.

in the biosorption with increase in pH implies that ion-exchange process is involved.

The reaction involved the biosorption of metal ion (represented as M^{x+}) from the liquid phase to the solid phase, the biosorbent with lone pair of electron (represented as Ä) and can be considered as a reversible reaction with an equilibrium

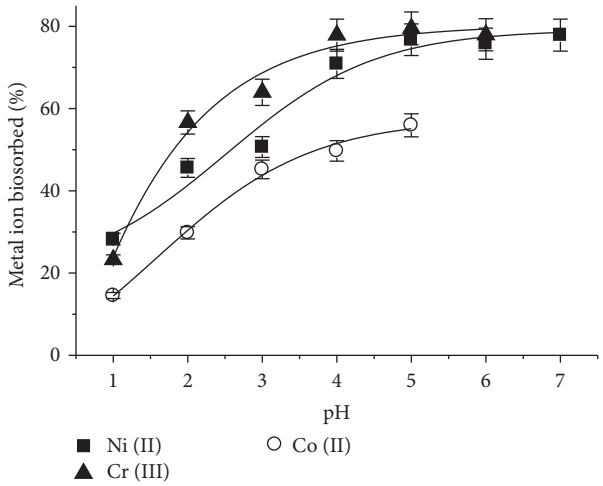


Figure 2: pH dependence profile for the biosorption of Ni(II), Cr(III), and Co(II) using *Acalypha hispida* leaf.

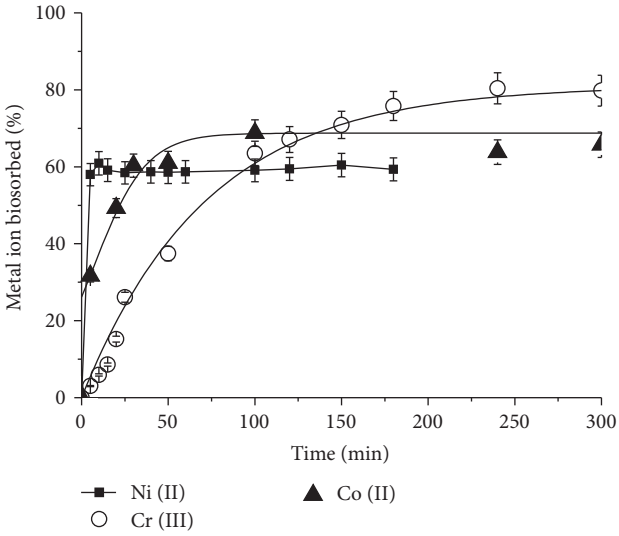


Figure 3: Contact time dependence profile for the biosorption of Ni(II), Cr(III), and Co(II) using *Acalypha hispida* leaf.

being made between the two phases as schematically shown below for a divalent metal ion in solution:

$$\ddot{A} + M^{2+} \rightleftharpoons A - M. \quad (1)$$

3.3. Biosorption Kinetics. Figure 3 illustrates the dynamic biosorption process of the three metal ions on *Acalypha hispida* leaf. It is observed that the biosorptive quantities of the three metal ions on the leaf increase with increasing contact time. In each case, biphasic kinetics are observed: an initial rapid stage (fast phase) where biosorption is fast and contributes to equilibrium uptake and a second stage (slow phase) whose contribution to the metal ion biosorbed is relatively smaller. The fast phase is the instantaneous biosorption stage, it is assumed to be caused by external biosorption of metal ion to the biomass surface. The second phase is a gradual biosorption stage, whose is diffusion rate is controlled. Finally, the biosorption sites are used up, the uptake of the metal ion reached equilibrium. This phase mechanism has been suggested to involve two diffusion processes, external and internal, respectively [20]. The biosorption of each of the three metal ions eventually achieves equilibrium although their rates of uptake and times of reaching equilibrium are different. This might be due to the differences in hydrated ionic sizes of the metal ions [21].

In order to establish the mechanism of the biosorption of Ni(II), Cr(III), and Co(II) on *Acalypha hispida* four kinetic models were applied to the kinetic data obtained. These are the pseudo-first-order, the pseudo-second-order, the Elovich kinetic model, and the Intraparticle diffusion model equations. One of such models is the Lagergren pseudo-first-order model which considers that the rate of occupation of the biosorption sites is proportional to the number of the unoccupied sites [17]:

$$\text{rate} = -\frac{d[A]}{dt} = k[A]^n. \quad (2)$$

Which can also be written as

$$\frac{d}{d_t} q_t = k_1 (q_e - q_t). \quad (3)$$

Integrating between the limits $q_t = 0$ at $t = 0$ and $q_t = q_t$ at $t = t$, we obtain

$$\log \left[\frac{q_e}{(q_e - q_t)} \right] = \frac{k_1}{2.303} t. \quad (4)$$

This can be rearranged to obtain a linear form:

$$\log (q_e - q_t) = \log q_e - \frac{k_1}{2.303} t, \quad (5)$$

where k_1 is the Lagergren rate constant of the biosorption (min^{-1}); q_e and q_t are the amounts of metal ions sorbed (mg g^{-1}) at equilibrium and at time t, respectively. The plot of $\log(q_e - q_t)$ versus t for the biosorption of metal ions on the biomass at initial concentration of $100\,\text{mgL}^{-1}$ did not give a straight line implying that the process does not follow first-order kinetic model. The data was equally subjected to the pseudo-second-order kinetic model. The pseudo-second-order kinetic model is represented as

$$\frac{d}{d_t} q_t = k_2 (q_e - q_t)^2. \quad (6)$$

On integrating between boundary conditions, we have

$$\frac{1}{q_e - q_t} = \frac{1}{q_e} + k_2 t. \quad (7)$$

On rearrangement, we have

$$\frac{t}{q_t} = \frac{1}{k_2 q_e^2} + \frac{1}{q_e} t, \quad (8)$$

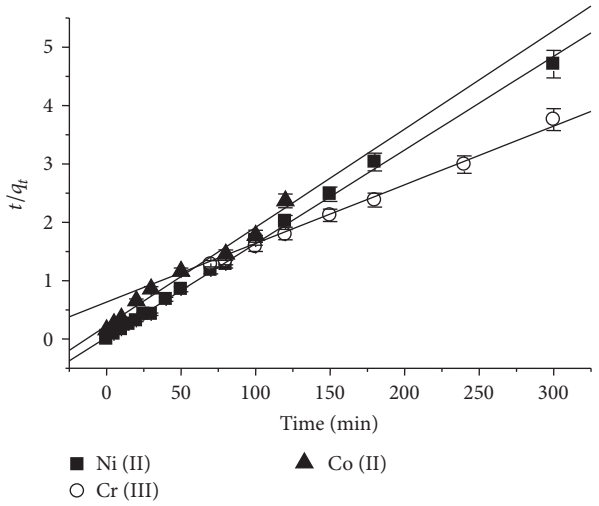


Figure 4: Pseudo-second-order kinetic plot for the biosorption of Ni(II), Cr (III), and Co (II) using *Acalypha hispida* leaf.

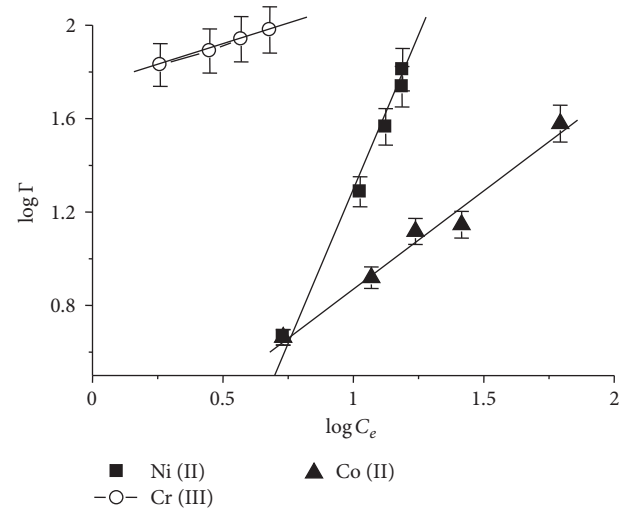


Figure 5: Freundlich isotherm for the biosorption of Ni(II), Cr(III), and Co(II) using *Acalypha hispida* leaf.

Table 2: Parameters of the pseudo-second-order kinetic model for the biosorption of Ni(II), Cr(III), and Co(II) using *Acalypha hispida* leaf.

Metal ion	k_2 (g·mg^{-1}·min^{-1})	q_e (mg·g^{-1})	R^2	S.D.
Ni(II)	8.395×10^{-3}	62.383	0.998	0.06133
Cr(III)	1.224×10^{-4}	107.296	0.963	0.12277
Co(II)	1.064×10^{-3}	60.096	0.977	0.11231

where k_2 is the equilibrium rate constant of pseudo-second-order biosorption process (g mg^{-1} min^{-1}). In the three metal ions under study, the pseudo-first-order kinetics did not fit the data obtained. However, plots of t versus t/q_t showed good fitness of experimental data with the pseudo-second-order kinetic model for different initial concentration of the three metal ions as presented in Figure 4.

The data were also subjected to the Elovish kinetic model given by

$$q_t = A + B \ln t, \tag{9}$$

and the intraparticle diffusion equation given as

$$R = K_s t^b. \tag{10}$$

The intraparticle diffusion equation has been used to indicate the behaviour of intraparticle diffusion as the rate limiting step in the biosorption process. R is the percent metal biosorbed, K_s is the intraparticle diffusion constant, t is the contact time, while b is the gradient of the linear plot. In the linear form, (10) turns to

$$\log R = b \log t + \log K_s. \tag{11}$$

The correlation coefficients obtained were found to be highest for the pseudo-second-order kinetics as it was found to be in excess of 0.9 as presented in Table 2.

On comparison of the values of R^2 for the experimental points, the pseudo-second-order kinetic model is the best kinetic model to predict the dynamic biosorption of Ni(II), Cr(III), and Co(II) on *Acalypha hispida* leaf similar to what was reported for banana leaf [22]. The result shows that the rate of biosorption of the metal ions is of the order Ni(II) > Co(II) > Cr(III). The biosorption capacity is in the order Cr(III) > Ni(II) ≈ Co(II). The differences observed in the rate of biosorption as well as in the biosorption capacity may be accounted for in terms of the differences in ionic charges and hydrated ionic sizes of the ions in solution [21].

3.4. Biosorption Isotherm. Figure 5 reports the Freundlich isotherms for the biosorption of Ni(II), Cr(III), and Co(II) on *Acalypha hispida* leaf. The equilibrium biosorption capacity increases with increase in metal ion concentration in each case.

The Freundlich and Langmuir isotherms were employed to calculate the biosorption capacity. The Freundlich isotherm is an empirical equation describing adsorption onto a heterogenous surface. The Freundlich isotherm is expressed as

$$\log \Gamma = \frac{1}{n} \log C_e + \log K_f, \tag{12}$$

where K and $1/n$ are the Freundlich constants related to the biosorption capacity and biosorption intensity of the biosorbent, respectively.

The linear form of the Langmuir equation is expressed as

$$\frac{1}{\Gamma} = \frac{1}{b_m} \frac{1}{C_e} + \frac{1}{\Gamma_m}, \tag{13}$$

where Γ, Γ_m, and b_m are the Langmuir parameters. The results show that the regression coefficients obtained for Freundlich isotherm are higher than for Langmuir isotherm. This implies that the biosorption is assumed to be a monolayer sorption with a heterogeneous energetic distribution of active sites, accompanied by interactions between biosorbed molecules

Table 3: Freundlich isothermal parameters the biosorption of Ni(II), Cr(III), and Co(II) using *Acalypha hispida* leaf.

Metal ion	$1/n$	K_f	R	S.D.
Ni(II)	2.4181	0.0742	0.9945	0.06
Cr(III)	0.3598	54.1627	0.9983	0.01
Co(II)	0.8432	1.0795	0.9885	0.06

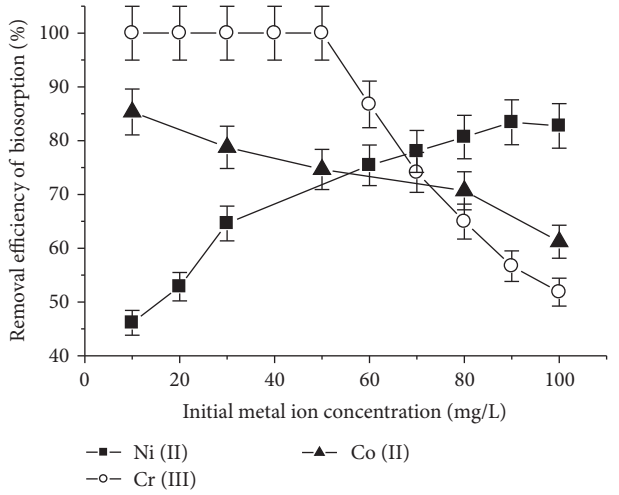


Figure 6: Efficiency plot for the biosorption of Ni(II), Cr(III), and Co(II) ions using *Acalypha hispida* leaf.

[1]. The Freundlich isothermal parameters for the biosorption are presented in Table 3.

3.5. Biosorption Efficiency. The result of the study on the effect of initial metal ion concentration on biosorption efficiency is shown in Figure 6. The plots show that the biosorption efficiency of the biomass reduces with increase in the initial metal ion concentration of Cr(III) and Co(II) which might be due to the fixed number of binding sites in the biosorbent having more ions than at lower concentration. On the other hand, the biosorption efficiency increased with the increase in initial metal ion concentration for Ni(II). The biosorption efficiency (E) for each metal ion was calculated as

$$E = 100\left(\frac{C_i - C_e}{C_i}\right), \tag{14}$$

where C_i and C_e are the initial and the equilibrium metal ion concentrations (mgL^{-1}), respectively.

3.6. Effect of Biomass Dosage on Biosorption. The effect of biomass dosage on biosorption capacity is reported in Figure 7. The general trend of increase in metal ion biosorbed with increase in biomass dosage indicates an increase in uptake due to more binding sites on the biomass available for biosorption. It was found that biosorption capacity increases with increase in dosage of the biosorbent. This is due to the fact that increase in biomass dosage leads to increase in the number of active sites available for biosorption. Hence, the

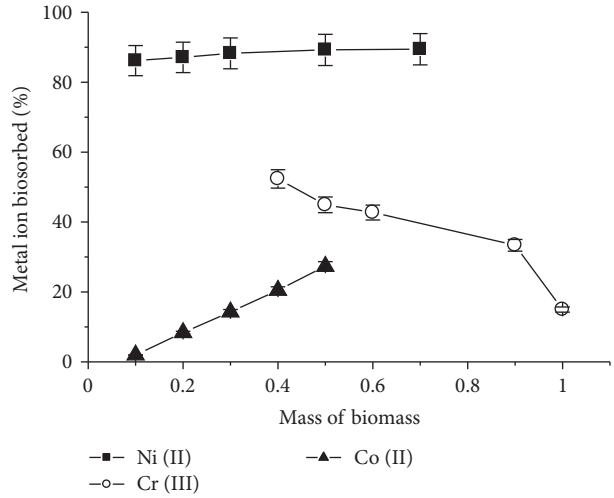


Figure 7: Effect of biomass dosage on the biosorption of Ni(II), Cr(III), and Co(II) using *Acalypha hispida* leaf.

amount of metal ions available for biosorption per gram of biosorbent will be less when the amount of biosorbent is increased. The difference in biosorption capacity q (mg g^{-1}) at the same initial metal ion concentration and contact time may also be attributed to the difference in their chemical affinities and ion exchange capacity, with respect to the chemical functional group on the surface of the biosorbent. This trend has been reported for other biosorbents [23].

3.7. Biosorption Thermodynamics. The biosorption of metal ions may involve chemical bond formation and ion exchange since temperature is a major parameter affecting them. The variation of temperature affects the biosorption of metal ions onto solid surfaces of biomass since the biosorption process is a reversible one. The nature of each side of the equilibrium determines the effect temperature has on the position of equilibrium. The side that is endothermic is favoured by an increase in temperature, while the contrary holds for the exothermic side. The corresponding free energy change was calculated from the relation [16, 24]:

$$\Delta G^\circ = -RT \ln K_c, \tag{15}$$

where T(K) is the absolute temperature. The equilibrium constant (K_c) was calculated from the following relationship:

$$K_c = \frac{C_{\text{ad}}}{C_e}, \tag{16}$$

where C_e and C_{ad} are the equilibrium concentrations of metal ions (mgL^{-1}) in solution and on biosorbent, respectively. Consequently, the thermodynamic behaviour of the biosorption of Ni(II), Cr(III), and Co(II) onto *Acalypha hispida* leaf was evaluated through the change in free energy (ΔG°), enthalpy (ΔH°), and entropy (ΔS°). The thermodynamic parameters like enthalpy and entropy were calculated using

Table 4: Thermodynamic parameters for the biosorption of Ni(II), Cr(III), and Co(II) onto *Acalypha hispida* leaf.

Metal ion	ΔH° (kJ mol^{-1})	ΔS° (J mol^{-1} K^{-1})	A (kJ mol^{-1}) (303 K)	A (kJ mol^{-1}) (318 K)
Ni(II)	4.63	17.029	7.15	7.32
Cr(III)	8.26	29.336	10.77	10.94
Co(II)	6.95	16.199	9.47	9.64

van't Hoff equation [6, 10]. The change in free energy is related to other thermodynamic properties as

$$\Delta G^\circ = \Delta H^\circ - T\Delta S^\circ,$$
$$\ln K_c = \frac{\Delta S^\circ}{R} - \frac{\Delta H^\circ}{RT}, \quad (17)$$

where T is the absolute temperature (K); R is the gas constant (8.314 J·mol^{-1}·K^{-1}). ΔH° (J·mol^{-1}) and ΔS° (J·mol^{-1}·K^{-1}) were calculated from the slope and intercept of the linear plot of $\ln K_c$ versus $1/T$, respectively. The thermodynamic parameters obtained for this study are presented in Table 3.

The thermodynamic parameters (free energy (ΔG°), enthalpy (ΔH°), and entropy (ΔS°)) for the biosorption of the metal ions were determined by the application of (15) and (16) as presented in Table 4. In general, the change of standard free energy for physisorption is in the range of −20 to 0 kJ mol^{-1} and for chemisorption varies between −80 and −400 kJ mol^{-1} [25, 26]. In the present study, the overall ΔG° (as shown in Figure 8) has values ranging from −1.5 to 2.25 kJ mol^{-1}. These results correspond to a spontaneous physical adsorption of the metal ions, indicating that this system does not gain energy from external resource [25, 27]. The decrease in ΔG° with increase in temperature indicates more efficient biosorption at higher temperature. The order of spontaneity of the biosorption process was found to be Cr(III) > Ni(II) > Co(II). The positive value of enthalpy change (ΔH°) indicates the endothermic nature of the biosorption process, while negative value implies exothermic process. The positive values of ΔH° for the biosorption of the three metal ions suggest an endothermic nature of each biosorption process. This is also supported by the increase in the value of biosorption capacity of the biosorbent with rise in temperature. The positive value of ΔH° indicates the presence of an energy barrier in the biosorption process. Similarly, the ΔS° values for Ni(II) and Co(II) are positive indicating increase in randomness during the biosorption process for these metal ions. These positive values of ΔS° observed for the biosorption of the three metal ions showed an increase in randomness at the solid/solution interface during their biosorption. The positive values of ΔS° suggest an increase in randomness at their solid/liquid interface, and it implies that significant changes occur in the internal structure of the adsorbents through the adsorption [25]. Furthermore, the magnitude of activation energy (A) gives an idea about the type of adsorption which is mainly diffusion-controlled process (not diffusivity of solute through micropore wall surface of a particle) or chemical reaction processes [28]. Energies of activation, A, below 42 kJ/mol indicate diffusion-controlled processes, and higher values

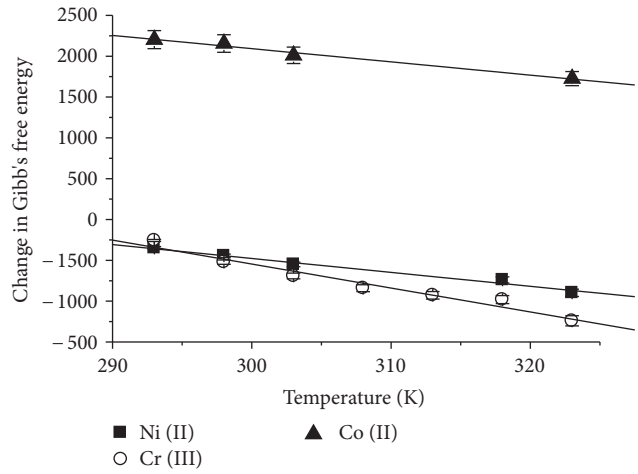


Figure 8: Thermodynamic plots for the biosorption of Ni(II), Cr(III), and Co(II) onto *Acalypha hispida* leaf.

give chemical reaction-based processes. Therefore, energy of activation, A, has been calculated as per the following relation:

$$A = \Delta H^\circ + RT. \quad (18)$$

The values of A at two different temperatures have been tabulated in Table 4. In this study, the activation energy (A) values were less than 42 kJ mol^{-1} indicating diffusion-controlled adsorption processes.

4. Conclusions

In this work we have studied the biosorption of Ni(II), Cr(III), and Co(II) by *Acalypha hispida* leaf under various conditions. The biosorption of each was influenced by each of the parameters investigated. The pH has much effect on the biosorption of these metal ions from aqueous solutions. The rate of the biosorption of these metal ions followed pseudo-second-order kinetic model. The sorption isotherms of these metal ions onto the biosorbent are better represented by the Freundlich isotherm model. The thermodynamic study shows that the biosorption of each of Ni(II), Cr(III), and Co(II) was spontaneous in the order Cr(III) > Ni(II) > Co(II). The order of disorderliness is Cr(III) > Ni(II) ≈ Co(II).

References

[1] B. Y. M. Bueno, M. L. Torem, F. Molina, and L. M. S. de Mesquita, "Biosorption of lead(II), chromium(III) and copper(II) by R. opacus: equilibrium and kinetic studies," *Minerals Engineering*, vol. 21, no. 1, pp. 65–75, 2008.

[2] N. A. A. Babarinde, J. O. Babalola, A. O. Ogunfowokan, and A. C. Onabanjo, "Kinetic, equilibrium, and thermodynamic studies of the biosorption of cadmium (II) from solution by Stereophyllum radiculosum," *Toxicological and Environmental Chemistry*, vol. 91, no. 5, pp. 911–922, 2009.

[3] N. A. A. Babarinde and J. O. Babalola, "Kinetic, Equilibrium and Thermodynamic studies of the biosorption of Cd(II) and Pb(II) from solutions using Siam leaf (Chromolaena odorata)," *International Review of Chemical Engineering*, vol. 2, no. 1, pp. 18–24, 2010.

[4] P. Chakravarty, N. S. Sarma, and H. P. Sarma, "Biosorption of cadmium(II) from aqueous solution using heartwood powder of *Areca catechu*," *Chemical Engineering Journal*, vol. 162, no. 3, pp. 949–955, 2010.

[5] Y. Liu, X. Sun, and B. Li, "Adsorption of Hg^{2+} and Cd^{2+} by ethylenediamine modified peanut shells," *Carbohydrate Polymers*, vol. 81, no. 2, pp. 335–339, 2010.

[6] O. D. Uluozlu, A. Sari, and M. Tuzen, "Biosorption of antimony from aqueous solution by lichen (*Physcia tribacia*) biomass," *Chemical Engineering Journal*, vol. 163, no. 3, pp. 382–388, 2010.

[7] J. Zhang and A. Wang, "Adsorption of Pb(II) from aqueous solution by chitosan-g-poly(acrylic acid)/attapulgite/sodium humate composite hydrogels," *Journal of Chemical and Engineering Data*, vol. 55, no. 7, pp. 2379–2384, 2010.

[8] K. Vijayaraghavan and R. Balasubramanian, "Single and binary biosorption of cerium and europium onto crab shell particles," *Chemical Engineering Journal*, vol. 163, no. 3, pp. 337–343, 2010.

[9] L. D. Fiorentin, D. E. G. Trigueros, A. N. Módenes et al., "Biosorption of reactive blue 5G dye onto drying orange bagasse in batch system: kinetic and equilibrium modeling," *Chemical Engineering Journal*, vol. 163, no. 1-2, pp. 68–77, 2010.

[10] R. Qu, Y. Zhang, C. Sun et al., "Adsorption of Hg(II) from an aqueous solution by silica-gel supported diethylenetriamine prepared via different routes: kinetics, thermodynamics, and isotherms," *Journal of Chemical and Engineering Data*, vol. 55, no. 4, pp. 1496–1504, 2010.

[11] T. Basu, K. Gupta, and U. C. Ghosh, "Equilibrium and thermodynamics on arsenic(III) sorption reaction in the presence of background ions occurring in groundwater with nanoparticle agglomerates of hydrous iron(III) + chromium(III) mixed oxide," *Journal of Chemical and Engineering Data*, vol. 55, no. 5, pp. 2039–2047, 2010.

[12] B. Reiersen, B. T. Kiremire, R. Byamukama, and Ø. M. Andersen, "Anthocyanins acylated with gallic acid from chenille plant, *Acalypha hispida*," *Phytochemistry*, vol. 64, no. 4, pp. 867–871, 2003.

[13] S. Okorondu, T. Sokari, M. Okorondu, and E. Chinakwe, "Phytochemical and antibacterial properties of Acalypha hispida leaves," *International Journal of Natural and Applied Sciences*, vol. 5, no. 2, pp. 34–43, 2009.

[14] P. A. Onocha, G. K. Oloyede, and Q. O. Afolabi, "Phytochemical investigation, cytotoxicity and free Radical scavenging activities of non-polar fractions of *Acalypha hispida* (leaves and twigs)," *EXCLI Journal*, vol. 10, pp. 1–8, 2011.

[15] S. Pradhan, S. Singh, and L. C. Rai, "Characterization of various functional groups present in the capsule of Microcystis and study of their role in biosorption of Fe, Ni and Cr," *Bioresource Technology*, vol. 98, no. 3, pp. 595–601, 2007.

[16] X. F. Sun, S. G. Wang, X. W. Liu et al., "Biosorption of Malachite Green from aqueous solutions onto aerobic granules: kinetic and equilibrium studies," *Bioresource Technology*, vol. 99, no. 9, pp. 3475–3483, 2008.

[17] N. Ertugay and Y. K. Bayhan, "Biosorption of Cr (VI) from aqueous solutions by biomass of *Agaricus bisporus*," *Journal of Hazardous Materials*, vol. 154, no. 1–3, pp. 432–439, 2008.

[18] K. Vijayaraghavan, T. V. N. Padmesh, K. Palanivelu, and M. Velan, "Biosorption of nickel(II) ions onto *Sargassum wightii*: application of two-parameter and three-parameter isotherm models," *Journal of Hazardous Materials*, vol. 133, no. 1–3, pp. 304–308, 2006.

[19] T. Akar, S. Tunali, and A. Çabuk, "Study on the characterization of lead (II) biosorption by fungus *Aspergillus parasiticus*," *Applied Biochemistry and Biotechnology*, vol. 136, no. 3, pp. 389–406, 2007.

[20] Y. Wu, L. Zhang, C. Gao, J. Ma, X. Ma, and R. Han, "Adsorption of copper ions and methylene blue in a single and binary system on wheat straw," *Journal of Chemical and Engineering Data*, vol. 54, no. 12, pp. 3229–3234, 2009.

[21] J. Kielland, "Effective diameters of unhydrated and hydratedions," *Journal of American Chemical Society*, vol. 59, pp. 1675–1678, 1937.

[22] N. A. A. Babarinde, J. O. Babalola, J. Adegoke, U. Maraizu, T. Ogunbanwo, and F. Ogunjinrin, "Kinetic, equilibrium and thermodynamic studies of the biosorption of Ni(II), Cr(III) and Co(II) from aqueous solutions using banana (Musa acuminata) leaf," *International Journal of Physical Sciences*, vol. 7, no. 9, pp. 1376–1385, 2012.

[23] M. A. Miranda, P. Dhandapani, M. H. Kalavathy, and L. R. Miranda, "Chemically activated Ipomoea carnea as an adsorbent for the copper sorption from synthetic solutions," *Adsorption*, vol. 16, no. 1-2, pp. 75–84, 2010.

[24] G. de la Rosa, H. E. Reynel-Avila, A. Bonilla-Petriciolet et al., "Biosorption of chromium species by aquatic weeds: kinetics and mechanism studies," *Journal of Hazardous Materials*, vol. 152, pp. 100–112, 2008.

[25] V. Vimonses, S. Lei, B. Jin, C. W. K. Chow, and C. Saint, "Kinetic study and equilibrium isotherm analysis of Congo Red adsorption by clay materials," *Chemical Engineering Journal*, vol. 148, no. 2-3, pp. 354–364, 2009.

[26] T. K. Sen, S. Afroze, and H. M. Ang, "Equilibrium, kinetics and mechanism of removal of methylene blue from aqueous solution by adsorption onto pine cone biomass of pinus radiata," *Water, Air and Soil Pollution*, vol. 218, no. 1–4, pp. 499–515, 2011.

[27] F. Arias and T. K. Sen, "Removal of zinc metal ion (Zn^{2+}) from its aqueous solution by kaolin clay mineral: a kinetic and equilibrium study," *Colloids and Surfaces A*, vol. 348, no. 1–3, pp. 100–108, 2009.

[28] M. M. Abd EI-Latif, A. M. Ibrahim, and M. F. EI-Kady, "Adsorption equilibrium, kinetics and thermodynamics of methylene blue from aqueous solutions using biopolymer oak sawdust composite," *American Journal of Science*, vol. 6, no. 6, pp. 267–283, 2010.